

Acoustic Emission in Single Crystals of Ice

Jérôme Weiss^{*,†} and Jean-Robert Grasso[‡]

Laboratoire de Glaciologie et Géophysique de l'Environnement, UPR CNRS 5151, BP 96,
38402 St. Martin D'Hères Cedex, France, and LGIT, Observatoire de Grenoble, BP 53X,
38041 Grenoble, France

Received: October 11, 1996; In Final Form: February 5, 1997[®]

The dislocation dynamics during the creep deformation of single crystals of ice Ih was studied using acoustic emission (AE) measurements. The AE activity was recorded during uniaxial compression and torsion creep tests. The results were interpreted in terms of dislocation dynamics with the help of an AE source model relating the amplitude of an acoustic event to the number of dislocations involved in the event and to their velocity. This model was first validated by a comparison between the global AE activity and the global strain rate. Then, it was possible to evaluate the density of moving dislocations during creep deformation. Two regimes were revealed. Without significant polygonization, the density of mobile dislocations, deduced from AE, was proportional to the stress, but increased much faster after polygonization, in agreement with theoretical arguments. Finally, the power law distributions observed for AE amplitudes, the slow driving process, the very large number of interacting dislocations involved, argued for the dislocation dynamics to be a new example of a class of nonlinear dynamics defined as a self-organized critical state (SOC). It would imply that, from a global point of view, the creep of ice single crystals is a marginally stable state rather than a steady-stable state.

Introduction

In solid materials, sudden local changes of inelastic strain generate acoustic emission (AE) waves. The sources can be dislocation motion, twinning, or crack nucleation and propagation.¹ Two typical forms of AE are associated with dislocation motion: continuous emission and individual events or swarms. Continuous emission is characterized by an increase of the AE background level with increasing strain rate. It results from the non-cooperative motion at low velocity of several dislocations during plastic deformation, and the signal is similar to noise.² On the other hand, events or swarms arise from high-velocity dislocation moves (plastic instabilities), likely during cooperative motion of dislocation groups, as in a dislocation breakaway or the activation of a Frank–Read source.^{2,3} Therefore, AE can be a useful tool for a statistical approach of dislocation dynamics.

Rheology of hexagonal ice Ih is highly plastically anisotropic.⁴ Basal glide is easier than nonbasal glide by at least 2 orders of magnitude. X-ray topography has been extensively used for the study of dislocations in ice,^{5,6} and dynamic parameters, such as the dislocation glide velocity, v , have been estimated.⁶ For stresses up to 1 MPa, a proportionality between v and the shear stress acting on the glide plane, τ , has been reported⁶ for a given temperature. However, observations are limited to samples with a low dislocation density, i.e., to low stresses, and it is questionable whether or not this holds for higher stresses. The goal of the present work is to study dislocation dynamics in single crystals of ice under creep, using AE measurements. The information collected is statistical, but can be obtained on high-dislocation-density samples, at large stresses.

Experimental Procedure

Laboratory-grown cylindrical ($R \approx 50$ mm; $L \approx 200$ mm) ice single crystals were prepared from distilled, deionized, and degassed water.⁷ When the c -axis of the seed (and so of the crystal) was parallel or perpendicular to the cylindrical axis of the mold, the internal stresses inside the growing crystal were small, and the single crystal was of good quality without visible (under cross-polarizers) polygonization or subboundaries. On the other hand, single crystals with an inclined c -axis (with respect to the axis of growth) were of lower quality and contained some detectable dislocation walls or subboundaries. These differences in the initial substructure led to differences in the dislocation dynamics under creep (see below).

Two kinds of creep experiments were performed at -10 °C:

(i) The first is uniaxial compression creep experiments with different steps of stress, on single crystals with the c -axis roughly parallel to the compression axis (i.e., a low resolved shear stress on the basal plane) or with the c -axis at about 45° to the compression axis (i.e., a high resolved shear stress on the basal plane). A strain–time curve obtained in the first case is represented in Figure 1. A constant strain rate is reached soon after the beginning of each loading step. This suggests the interpretation of data indeed applied to a nominally “stable” dislocation dynamics.

(ii) The second is a torsion creep test (see Duval⁸ for details about the experimental method) with different steps of constant momentum. During this experiment the basal plane of the single crystal was roughly parallel to the torsion plane.

A piezoelectric transducer with a frequency bandwidth of 0.1–1 MHz was fixed by fusion/freezing on the side of the samples. This ensured an excellent coupling between the material and the transducer. The signals registered were individual events or swarms. The event amplitude threshold was adjusted to about 5 dB above the noise level, and the envelope “dead time” (the minimum time between to successive events), fixed at 50 μ s. The dynamic range between the

* Author to whom correspondence should be addressed. E-mail: weiss@glaciog.ujf-grenoble.fr.

[†] UPR CNRS 5151.

[‡] Observatoire de Grenoble.

[®] Abstract published in *Advance ACS Abstracts*, June 1, 1997.

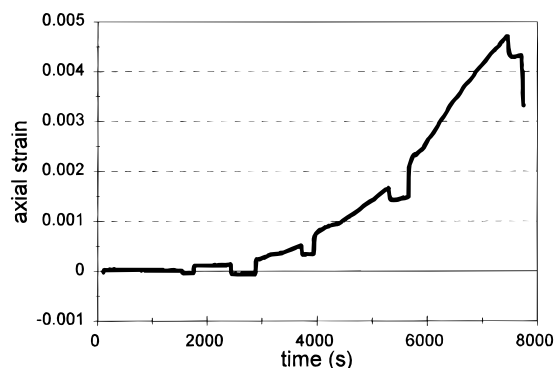


Figure 1. Strain–time curve for an uniaxial compression creep test on a single crystal with the *c*-axis roughly parallel to the compression axis. The loading steps correspond to compressive stresses σ_∞ of 0.6, 2.4, 3.15, 4.1, and 5.7 MPa.

threshold and the maximum amplitude recorded was 70 dB, i.e., $3^{1/2}$ orders of magnitude. We recorded amplitudes of AE events for each loading step.

AE Source Model. Thanks to the perfect transparency of the ice single crystals, it was easily verified that no cracks nucleated during the creep tests. Therefore, the only possible AE source appears to be dislocation motion during viscoplastic deformation. As a first step, we propose a crude model that relates the AE signal amplitude to high-velocity dislocation motion. This model will be validated in a second step by comparison between AE activity and global strain rate and then used, in a third step, to study different aspects of dislocation dynamics.

The remote resolved shear stress on the basal planes, τ_∞ , applied during the experiments, was always lower than 0.3 MPa. At -10°C , the corresponding dislocation velocity is approximately $3\text{--}5\ \mu\text{m}\cdot\text{s}^{-1}$. At this velocity, a dislocation line will move over a distance \mathbf{B} (Burgers' vector) in about 5×10^{-5} s. Therefore, the frequency of the associated signal will be in the range 10–100 kHz, i.e., below the frequency range of the transducer. So, the recorded signals are unlikely the result of dislocation motion at these velocities. It will be shown now that AE is more likely related to dislocation motion at higher velocity in stress concentration regions. Two main phenomena can support sudden acceleration and high-velocity motion of dislocations (instabilities) during plastic deformation of single crystals.^{2,3} The activation of a Frank–Read source (FRS) or the breakaway of a pileup of dislocations. Both processes can produce synchronized moves of several dislocations, resulting in a unique AE swarm.

FRS have been observed in ice.⁹ FRS are activated where stress concentrations are present. The generation of dislocation loops from the FRS relaxes stress concentrations, so the FRS deactivates. Calculations¹⁰ suggested very short times ($\sim 10^{-9}$ s) for dislocation loop formation from a FRS. However, frictional drag on dislocation motion would reduce the frequency of loops formation.¹⁰ The formation of one or several loops could lead to AE in the frequency range explored.

The second possible mechanism of AE during creep of single crystals is the dislocation breakaway. Even a carefully grown single crystal will contain, before deformation, a stable network of grown-in dislocations organized along dislocation walls or low-angle boundaries.⁵ Some subboundaries, parallel to the *c*-axis, were detectable under cross-polarizers on some single crystals prepared for this work (see above). During creep deformation, dislocations moving on the basal planes will pile-up against the preexisting walls or subboundaries. Because of the very low impurity content of the samples,⁷ the pileup of

dislocations against other kinds of obstacles is unlikely. A dislocation wall exerts a force \mathbf{F}_{sb} on the head of the pileup. At the equilibrium, \mathbf{F}_{sb} is balanced by the force \mathbf{F}_{p} exerted by the pileup on the leading dislocation. The number of dislocations in the pileup, n_{p} , increases as deformation increases, until \mathbf{F}_{p} exceeds \mathbf{F}_{sb} . Then, the dislocations of the head of the pileup will then pass suddenly through the obstacle (the dislocation wall) at a velocity \mathbf{v} , under the action of the stress field created by the pileup, of the order of¹¹ $n_{\text{p}}\tau$. It is worth emphasizing here the possible interactions between dynamics of FRS and pileups. As an example, dislocations emitted from a FRS can pile-up against an obstacle, and the back-stress from the pileup on the source can stop the FRS activity¹² before pileup breakaway.

The amplitude of the signal s (in volts), resulting from the cooperative motion of n dislocations, is of the form^{2,13}

$$s = k \frac{nL\mathbf{B}\mathbf{v}t_0}{d} \quad (1)$$

where k is a coefficient depending on the material properties and the piezoelectric constant of the transducer, \mathbf{B} is the Burgers' vector, L is the length of the n moving dislocations, \mathbf{v} is their velocity (supposed constant in time and space during the event), and d is the distance source/transducer (supposed large compare to L). t_0 is the time needed for the acoustic waves to travel from one side of the transducer to the other one and is considered here to be constant. The term $1/d$ represents the attenuation of the acoustic wave. In the case of a FRS, nt_0 represents the production rate of dislocation loops from the source. The key assumption here is to relate the amplitude of the signal to the number and velocity of moving dislocations in the group. This is a reminder of the well-known Orowan's relation for the shear strain rate of a single crystal:

$$d\gamma/dt = \rho_{\text{m}}\mathbf{B}\mathbf{v} \quad (2)$$

where ρ_{m} is the density of mobile dislocations. So, in a sense, the AE amplitude s is proportional to the local strain rate during the event (in (2), nL corresponds to ρ_{m}). From the distributions of AE amplitudes, we now introduce the rate \dot{A} , which is the sum of the amplitudes s of all of the events registered during one loading step, divided by the duration of the step, t_s :

$$\dot{A} = \frac{\int_{s_{\text{min}}}^{s_{\text{max}}} N(s)s\,ds}{t_s} \quad (3)$$

where $N(s)$ is the number of events with an amplitude between $s - ds$ and $s + ds$.

\dot{A} is a measure of the global AE activity during a loading step. If the high-velocity dislocation moves detected by AE are representative of the global dislocation dynamics, we can expect a proportionality between \dot{A} and $d\gamma/dt$, the strain rate measured at the end of the loading step. This will be used to check the validity of the proposed AE source model.

If the proportionality between \mathbf{v} and the local shear stress acting on the basal plane,⁶ τ , holds for large stresses, the amplitude s of an event (or a swarm) should be, from (1), proportional to $nL\tau$. On average, the stress concentrations in the material are proportional to the applied stress. Therefore, averaging over the full set of AE events, \dot{A} should be linearly related to $\rho_{\text{m}}\tau_\infty$. \dot{A}/τ_∞ thus becomes a direct measure of ρ_{m} .

Results and Discussion

A typical cumulative distribution of AE amplitudes, corresponding to one loading step, is represented in Figure 2 in a

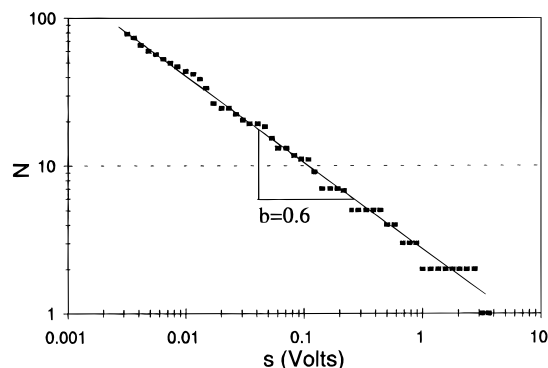


Figure 2. AE amplitude distribution for a uniaxial compression test (step at $\sigma_{\infty} = 4.1$ MPa) on a vertical c -axis single crystal.

log-log frame. A power-law distribution was systematically observed for each step of each test:

$$\log_{10} N_{\text{cum}} = a - b \log_{10} s \quad (4a)$$

or

$$N_{\text{cum}} = As^{-b} \quad (4b)$$

where N_{cum} is the number of events of amplitude larger than s . Observed b values were in the range 1–0.5.

This type of distribution ensures that the observed evolutions of \dot{A} with external parameters, like stress or strain rate (see below), are independent of the chosen amplitude threshold s_{min} .

Validation of the AE Source Model. In the case of uniaxial compression tests, the values of \dot{A} measured for the same uniaxial compressive stress, σ_{∞} , were at least 2 orders of magnitude larger for single crystals with an inclined c -axis than for crystals with a quasi-vertical c -axis. It supports the hypothesis that relates \dot{A} to dislocation motion driven by the shear stress acting on the basal planes, which is very small when the c -axis is almost parallel to the compression axis.

The linear relationship between \dot{A} and $d\gamma/dt$ seems to be verified for a uniaxial compression test (Figure 3a) as well as for a torsion test (Figure 3b). These two observations support the AE source model proposed. However, it should be noted in Figure 3b that \dot{A} was much larger than expected for the last step of the torsion test. This could be related to an evolution of the internal substructure of the single crystal (see below).

Density of Moving Dislocations. In Figure 4a is plotted the evolution of \dot{A}/τ_{∞} (a measure of ρ_m) with τ_{∞} , for a compression test on a vertical c -axis single crystal. A linear relationship is observed. Because of the plastic anisotropy of ice Ih, the creep of single crystals of good quality is controlled by basal glide.⁴ Therefore, the density of moving dislocations, ρ_m , should be theoretically proportional to $1/l$, where l is a length characterizing the spatial distribution of dislocations, namely, the distance between parallel slip lines. On the other hand, the internal stress field of the dislocations varies with $1/r$ (r , distance from the dislocation). So, l should be inversely proportional to the applied stress because of the interactions between dislocations.¹⁴ Therefore, ρ_m will be proportional to τ_{∞} , as observed on Figure 4a. Such a relation also agrees with eq 2, and an exponent of 2 in the Norton's law ($d\gamma/dt \propto \tau_{\infty}^2$) for the creep of single crystals of ice⁴ [indeed, if $\dot{\gamma} \propto \tau$, then $d\gamma/dt = \rho_m \times \mathbf{B} \times \tau_{\infty} \propto \tau_{\infty}^2$, so $\rho_m \propto \tau_{\infty}$].

In this way we agree that AE measurements allow estimation the density of moving dislocations during the viscoplastic deformation of ice single crystals. Moreover, the observed agreement is an indirect indication in favor of a proportionality between $\dot{\gamma}$ and τ , even at large stresses.

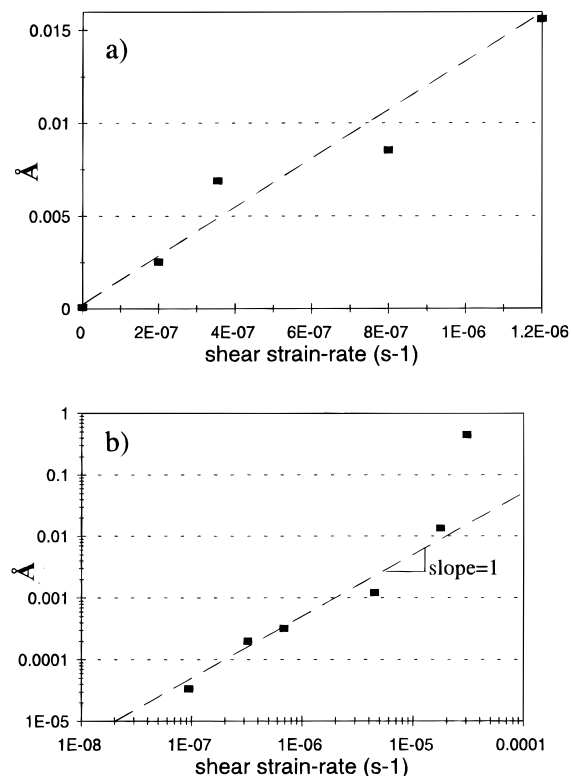


Figure 3. Evolution of the AE activity (parameter \dot{A}) with the shear strain rate (where, for example, $2\text{E}-07 = 2 \times 10^{-7}$): (a) for a uniaxial compression test on a vertical c -axis single crystal; (b) for a torsion test (a log-log frame is used because of the very large range of strain rates).

A linear relationship between \dot{A}/τ_{∞} (or ρ_m) and τ_{∞} was also observed for the torsion test up to a shear stress of about 0.2 MPa (Figure 4b, inset). However, at higher applied stresses, \dot{A}/τ_{∞} increased much faster than τ_{∞} (Figure 4b). A nonlinear increase of \dot{A}/τ_{∞} with τ_{∞} was also observed with an inclined c -axis single crystal under uniaxial compression. We propose this can be related to changes in the substructure, i.e., polygonization.

Polygonization. Depending on the initial quality of the single crystal and on the level of stress applied, it was possible to classify the experiments in two categories.

Experiments performed on single crystals without visible subboundaries were characterized by (i) \dot{A}/τ_{∞} (or ρ_m) $\propto \tau_{\infty}$ (Figure 4) (as explained above, this is consistent with the creep of single crystals controlled by basal glide), (ii) an almost unchanged substructure (observations performed after testing did not reveal subboundaries or polygonization; however, a more detailed analysis by another technique, such as X-ray topography, would be necessary to detect the onset of polygonization), and (iii) an unchanged b -value (relation 4a or 4b); the exponent of the AE amplitude distribution, for a given sample, was independent of stress).

On the other hand, the presence of detectable subboundaries before testing, as well as high stresses, favored polygonization during creep.¹² The dislocation climb velocity, v_c , increases with increasing stress ($v_c \propto \sigma$).^{12,14} At large stresses, some of the moving dislocations will be able to climb along the dislocation walls or to create new walls, leading to the following:

(i) A polygonization substructure is created. An evolution of the substructure was clearly detected on thin sections after testing. A high density of subboundaries was observed, generally more or less parallel to the initial c -axis, but organized in "cells" perpendicular to it. Once again, observations under

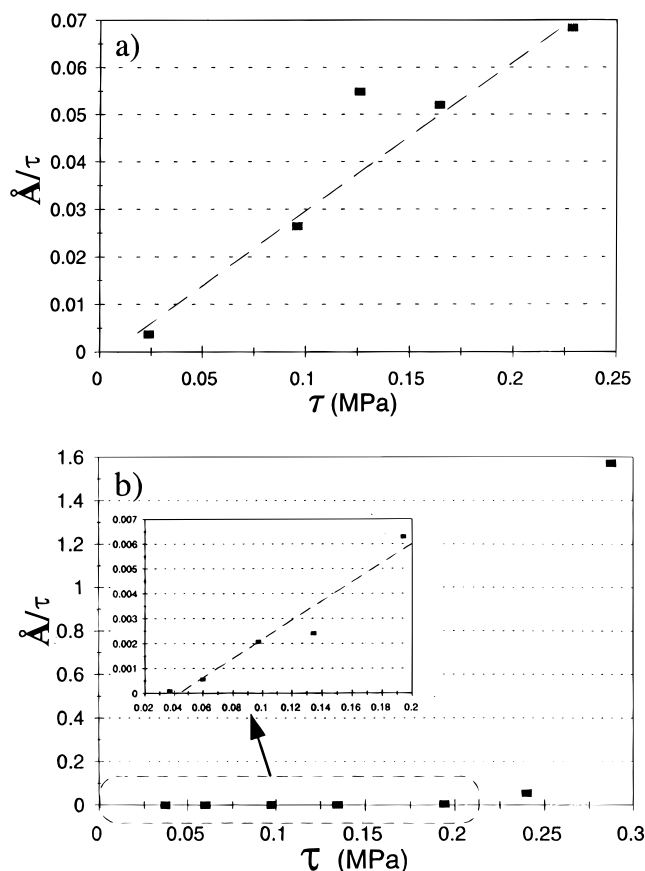


Figure 4. Evolution of \dot{A}/τ_∞ (a measure of ρ_m) with τ_∞ : (a) for an uniaxial compression test on a vertical c-axis single crystal; (b) for a torsion test (results for $\tau_\infty \leq 0.2$ MPa are detailed in the inset).

cross-polarizers were difficult, and X-ray topography would have been very useful for a detailed analysis.

(ii) A nonlinear increase of \dot{A}/τ_∞ with τ_∞ (Figure 4b) is observed. A theoretical dimensional argument similar to the one used in the case of basal glide without polygonization can be developed here. When creep is controlled by dislocation climb, with the formation of a *tridimensional* substructure, the (total) dislocation density, ρ , is proportional to $1/l^2$, where l is, once again, a length characterizing the spatial distribution of dislocations¹⁴ (the "subgrain size"). ρ is then proportional to the square of the stress, and so to the density of *mobile* dislocations, ρ_m , which is generally considered to be proportional to ρ .¹⁴ This is consistent with a nonlinear increase of \dot{A}/τ_∞ with τ_∞ (Figure 4b). Indeed, we are probably in a situation where the deformation is *controlled* by the climb process but primarily *due* to the activity of basal slip.^{4,15} Therefore, dislocation motion occurs essentially by basal glide, and ρ_m can still be estimated from the AE activity. As a matter of fact, \dot{A}/τ_∞ was observed to increase in τ_∞^m at large stresses, with m between 3 and 4, rather than equal to 2 (Figure 4b). Correspondingly, the exponent of the Norton's law should increase and become close to 3 ($d\gamma/dt \propto \tau_\infty^3$) [indeed, if the deformation is controlled by dislocation climb, one can write $d\gamma/dt \propto \rho_m \times \mathbf{B} \times \mathbf{v}_c$;¹⁴ if \mathbf{v}_c is proportional to the applied stress, and $\rho_m \propto \tau_\infty^2$, then $d\gamma/dt \propto \tau_\infty^3$], as for polycrystals.⁴ Such an increase was experimentally observed in our tests at high stress.

(iii) An evolution of the b value with τ_∞ is seen. During polygonization, the dislocation dynamics change. Dislocation climb along walls or subboundaries becomes possible, whereas new walls are formed. This leads to a reorganization of the internal stress field, and so to changes in the distribution of AE

amplitudes. A decrease of b with increasing stress was observed.

So, the measure of the parameters \dot{A} and b , determined from AE distributions, seems to allow detection of polygonization.

Dislocation Dynamics during Creep: A Self-Organized Critical System? We have shown that AE recorded during the creep of ice single crystals was associated with dislocation motion. Amplitude distributions systematically follow power-law distributions (Figure 2). A similar pattern is recovered for the distributions of AE events associated with crack dynamics, at a scale ranging from damage of laboratory rock samples¹⁶ (10^{-4} m) to earthquakes¹⁷ (10^5 m). Within this context, equation 4a is equivalent to the Gutenberg–Richter law observed for earthquakes.¹⁷ The power-law distributions of earthquakes in energy, space, and time domains were difficult to understand because earthquake dynamics appears as a complex, nonlinear system. Recently, theoretical statistical physics were proposed to rationalize this global dynamics within the concept of self-organized criticality¹⁸ (SOC).

SOC is admitted to be characterized by (i) power-law distributions, such as those observed for AE amplitudes during the creep of ice single crystals (Figure 2 and relations 4a and 4b); (ii) a slow external loading (the driving process) relatively to the velocity associated with the internal events (in our experiments, the local strain rates induced by the plastic instabilities (see above) are much larger than the global strain rates); (iii) a threshold dynamics (the activation of a FRS or a dislocation breakaway are launched above a local threshold stress); and (iv) a very large number of interacting local entities (here, the dislocations) (for a SOC system, the global dynamics is proposed to be driven by the long-range correlations between a large number of local entities, rather than by the properties or physical rules locally applied on such entities,¹⁸ and dislocations interact through their associated stress fields,¹² as cracks do (see, e.g., Kachanov¹⁹ for an analysis of crack interactions in elastic solids); this could explain that dislocation dynamics mimics damage and earthquake dynamics).

In this way, the dislocation dynamics during the creep of ice single crystals appears as a new example of SOC state. It is interesting to note that power-law statistics have been reported also for the stress drops associated with the Portevin–Le Chatelier plastic instabilities in Al–Mg alloys,²⁰ suggesting the relation between dislocation dynamics and SOC is not restricted to ice. From a global point of view, the creep of ice single crystals appears to be in an apparent steady-state behavior (see above and Figure 1). However, as we proposed dislocation dynamics to be a SOC state, we guessimate the system to be a complex, nonlinear, marginally stable system.¹⁸ In such a system, local events (plastic instabilities) are unpredictable in space, time, and energy, as they are for earthquake dynamics.

Conclusion

The AE activity of ice single crystals under compression or torsion creep was recorded and analyzed in terms of dislocation dynamics. An AE source model was presented, where individual AE events or swarms are the result of high-velocity motion of dislocations, during the activation of a Frank–Read source or the destruction of a pileup. This model was supported by a comparison between global AE activity and global strain rate.

AE measurements allow an estimate of the evolution of the density of mobile dislocations, ρ_m , during creep deformation. Two regimes were observed:

(i) For single crystals without initial visible subboundaries or dislocation walls and for low resolved shear stress (τ_∞) on

the basal planes, a linear relationship was observed between ρ_m , as deduced from AE, and τ_{∞} .

(ii) The presence of initial subboundaries, as well as high stresses, favored the polygonization process. The resulting tridimensional network of dislocations was invoked to explain the observed very strong increase of the AE activity (or ρ_m) with τ_{∞} ($\rho_m \propto \tau_{\infty}^3 - \tau_{\infty}^4$).

Finally, the power-law distributions observed for AE amplitudes suggest that the dislocation dynamics during creep of ice single crystals is a self-organized critical system, globally similar to the complexity of the brittle deformation of the earth crust.

Acknowledgment. We would like to thank D. Hantz and Y. Orenge for AE technical support, P. Duval and F. Lahaie for valuable discussion, and an anonymous reviewer for helpful comments. The single crystals were prepared by O. Brissaud. LGGE is a laboratory of the CNRS associated with Université J. Fourier, Grenoble.

References and Notes

- (1) Malen, K.; Bolin, L. *Phys. Stat. Sol.* **1974**, *61*, 637.
- (2) Rouby, D.; Fleischmann, P.; Duvergier, C. *Philos. Mag. A* **1983**, *47*, 671.
- (3) James, D. R.; Carpenter, S. H. *J. Appl. Phys.* **1971**, *42*, 4685.
- (4) Duval, P.; Ashby, M. F.; Andermann, I. *J. Phys. Chem.* **1983**, *87*, 4066.
- (5) Petrenko, V. F.; Whitworth, R. W. *CRREL Spec. Rep.* 94-12 **1994**.
- (6) Shearwood, C.; Whitworth, R. W. *Philos. Mag. A* **1991**, *64*, 289.
- (7) Thibert, E.; Dominé, F. Submitted for publication in *J. Phys. Chem.* **1996**.
- (8) Duval, P. *Ann. Geophys.* **1976**, *32*, 335.
- (9) Ahmad, S.; Shearwood, C.; Whitworth, R. W. In *Physics and Chemistry of Ice*; Maeno, Hondoh, Eds.; Hokkaido University Press, 1992; p 492.
- (10) Campbell, J. D.; Taylor, D. B. In *Stress Waves in Anelastic Solids*; Kolsky, H., Prager, W., Eds.; Springer-Verlag: Berlin, 1963; p 54.
- (11) Stroh, A. N. *Proc. R. Soc. Lond. A* **1954**, *223*, 404.
- (12) Friedel, J. *Dislocations*; Pergamon Press: Oxford, U.K., 1964.
- (13) Rouby, D.; Fleischmann, P.; Duvergier, C. *Philos. Mag. A* **1983**, *47*, 689.
- (14) Poirier, J. P. *Plasticité à Haute Température des Solides Cristallins*; (High Temperature Plasticity of Crystalline Solids); Eyrolles: Paris, 1976.
- (15) Castelnau, O.; Duval, P.; Lebensohn, R. A.; Canova, G. *J. Geophys. Res.* **1996**, *101*, 13851.
- (16) Scholz, C. H. *Bull. Seismol. Soc. Am.* **1968**, *58*, 399.
- (17) Gutenberg, B.; Richter, C. F. *Seismicity of the Earth and Associated Phenomena*; Princeton University Press: Princeton, NJ, 1954.
- (18) Bak, P.; Tang, C.; Wiesenfeld, K. *Phys. Rev. A* **1988**, *38*, 364.
- (19) Kachanov, M. *Adv. Appl. Mech.* **1994**, *30*, 259.
- (20) Lebyodkin, M. A.; Brechet, Y.; Estrin, Y.; Kubin, L. P. *Phys. Rev. Lett.* **1995**, *74*, 4758.